Correcting Non-Line-of-Sight Path Length Estimation for Ultra-Wideband Indoor Localization

Quoc-Tuong Ngo*, Pierre Roussel*, Bruce Denby†*, and Gerard Dreyfus*
*Sigma Laboratory - ESPCI ParisTech, Paris, France
†Université Pierre et Marie Curie, Paris, France
Email: Firstname.Lastname@espci.fr

***Abstract*—Ultra-Wideband technology provides accurate localization in indoor environments using time-of-arrival based ranging techniques; however, the positioning accuracy is degraded by non-line-of-sight conditions. In this work, the relation between the non-line-of-sight path length error and the obstacles on the path from transmitter to receiver is used as input to a new positioning algorithm to correct the corrupted measurements. Simulation and experimental results demonstrate that the proposed algorithm provides a significant improvement in positioning accuracy as compared to line-of-sight algorithms.**

***Index Terms*—Indoor localization, Ultra-Wideband, TOA, NLOS, Two Way Ranging, position estimation.**

I. Introduction

In recent years, the demand for accurate localization in indoor environments such as office buildings, department stores, and transportation facilities has increased dramatically. Since the coverage of the GPS signal is limited in indoor environments, various technologies, including RFID [1], Wi-Fi [2], and Bluetooth [3] have been proposed to provide better solutions. In this paper, Ultra-Wideband (UWB) technology developed by the IEEE 802.15 Task Group 4 is studied. The principal feature of such UWB systems is to provide not only low power consumption, but also precise indoor localization, to within 1 m for ranges below 300 m in Line of Sight (LOS) conditions [4].

A UWB positioning system can employ various ranging techniques using Received Signal Strength (RSS) [5], Time of Arrival (TOA) [6], Time Difference of Arrival (TDOA), or Angle of Arrival (AOA) [7]. In practice, TOA-based methods provide better position accuracy at lower cost, in comparison to RSS and AOA methods. Furthermore, unlike TDOA, a classical TOA ranging method can be implemented using the Two Way Ranging (TWR) technique, which does not require precise synchronization.

In the indoor environment, TOA based geolocation accuracy can be degraded by Non Line of Sight (NLOS) conditions. To mitigate NLOS propagation errors, the authors of [8] manually built a map of measurement noise and used it with a particle filter to improve position measurement accuracy. A disadvantage of this method is that creating such a map increases computational complexity. The present work outlines a simple technique that does not increase the complexity but significantly improves UWB localization performance. We first present the simple form of the NLOS path length error, which depends on the thickness of the obstacles and the intersection angle between them and the direct path. Then, a new positioning algorithm based on correcting raw TOA measurements for changes in phase velocity of radio waves passing through different media is presented, for the context of UWB ranging.

The paper is organized as follows. The next Section outlines the localization methods used in the proposed UWB system. The NLOS indoor location algorithm is introduced in Section III, while the experiments and the simulation results are presented in Section IV. A conclusion appears in the final Section.

978-1-4799-9858-6/15/$31.00

II. Methods

A. Two Way Ranging method

The basic protocol of the Two Way Ranging (TWR) technique is illustrated in Fig. 1. Typically, one node is chosen to act as a Tag, and the other as Anchor. A Tag first sends a Poll message to the Anchor and calls the corresponding send time T_{SP}. When the Anchor receives this Poll message, it records the receive time T_{RP}, sends a Response message back to the Tag, and notes its send response time T_{SR}. If the Tag receives the Response message, it records the received response time T_{RR}, and sets a future time T_{SF} at which to send the final message to the Anchor (all time measurements T_{SP}, T_{RR}, and T_{SF} are embedded in the Final message). With the final response message, the Anchor now has enough information to determine the one-way travel time T_t.

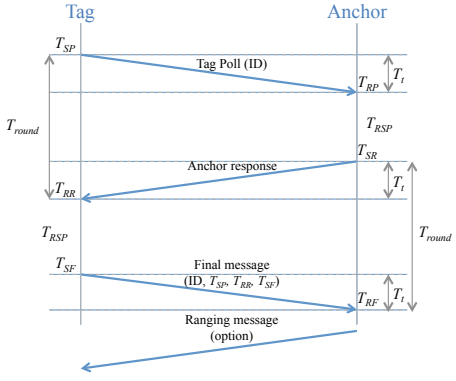

Fig. 1. Two Way Ranging protocol.

Considering the round trip travel time, the time of flight (TOF) is defined by

$$T_t = \frac{1}{4}\left(T_{round}^{Tag} - T_{RSP}^{Anchor} + T_{round}^{Anchor} - T_{RSP}^{Tag}\right) = \frac{1}{4}(2T_{RR} - T_{SP} - 2T_{SR} + T_{RP} + T_{RF} - T_{SF}). \quad (1)$$

If c is the signal propagation speed, the distance between the Tag and the Anchor is then given as

$$r = cT_t. \quad (2)$$

B. TOA-based positioning technique

For simplicity, TOA-based location in two-dimensional space (2-D) is considered here. The extension to three dimensions is straightforward. First, it is assumed that N Anchors are used to locate the position of a Tag on a 2-D floor plan. Denoting (x, y) as the true location of the Tag, (x_i, y_i) the location of the i^{th} known Anchor, and r_i the TWR-estimated distance between the Tag and the i^{th} Anchor, the estimated distance is given by

$$r_i = f_i + e_i, \text{ with } i = 1..N, \quad (3)$$

where $f_i(x, y) = \sqrt{(x - x_i)^2 + (y - y_i)^2}$ is the true distance between the Tag and the i^{th} Anchor, and e_i represents the error in the distance estimation.

There are many TOA-based localization techniques for LOS scenarios [9], and we consider, herein, the non linear least squares solution based on a first-order Taylor expansion due to its positioning accuracy obtained at convergence. The observed distance is then expressed in matrix form as

$$\mathbf{r} = \mathbf{f}(x_0, y_0) + \mathbf{G}\boldsymbol{\delta} + \mathbf{e}, \quad (4)$$

or

$$\mathbf{G}\boldsymbol{\delta} = \mathbf{h} - \mathbf{e}, \quad (5)$$

where

$$\mathbf{G} = \begin{bmatrix} \frac{\partial f_1}{\partial x} & \frac{\partial f_1}{\partial y} \\ \vdots & \vdots \\ \frac{\partial f_N}{\partial x} & \frac{\partial f_N}{\partial y} \end{bmatrix} = \begin{bmatrix} \frac{x - x_1}{f_1} & \frac{y - y_1}{f_1} \\ \vdots & \vdots \\ \frac{x - x_N}{f_N} & \frac{y - y_N}{f_N} \end{bmatrix},$$

$$\boldsymbol{\delta} = \begin{bmatrix} \Delta x \\ \Delta y \end{bmatrix}, \ \mathbf{h} = \begin{bmatrix} r_1 - f_1 \\ \vdots \\ r_N - f_N \end{bmatrix}. \quad (6)$$

Minimizing the sum of squared errors, weighted according to the covariance of the estimation errors, with respect to $\boldsymbol{\delta}$, one obtains:

$$\boldsymbol{\delta} = \left(\mathbf{G}^T\mathbf{R}^{-1}\mathbf{G}\right)^{-1}\mathbf{G}^T\mathbf{R}^{-1}\mathbf{h}, \quad (7)$$

where $\mathbf{R} = [\langle e_i, e_j \rangle]$ is the covariance matrix of the estimation error $\mathbf{e}$, and all matrices in equation (7) are computed with $x = x_0$ and $y = y_0$. If an initial estimate of the position (x_0, y_0) is available, equation (7) may be used to obtain $(x_0 + \Delta x, y_0 + \Delta y)$, and the process is repeated until convergence, i.e., Δx and Δy become sufficiently small according to some criterion.

C. Ultra-Wideband system

The experimental system employed uses the UWB transceiver chip DW1000 developed by Decawave [10]. Based on IEEE 802.15.4a, the real time localization system can locate the Tag position within a few tens of centimeters. The distances are determined by the TWR technique, where the TOA-based location is estimated by at least three Anchor positions.

III. NLOS INDOOR LOCATION ALGORITHM

A. NLOS path length estimation error

In an indoor environment, the signal from the source is usually unable to arrive at the receiver directly. Because of obstacles, walls for example, NLOS path lengths are overestimated by LOS estimation algorithms. At the same time, a main advantage of UWB for indoor location is its ability to penetrate through obstacles with little degradation of the UWB waveform. For a w-meter thick obstacle, the authors in [11] showed that an additional TOF delay is given by

$$\tau = \frac{w}{c}\left(\sqrt{\varepsilon_r \mu_r} - 1\right), \quad (8)$$

where c is speed of light, μ_r is the relative permeability, and ε_r is the relative permittivity of the obstacle. Therefore, if this delay is not taken into account, there occurs an error n_τ on the NLOS path length estimation

$$n_\tau = c\,\tau = w\left(\sqrt{\varepsilon_r \mu_r} - 1\right). \quad (9)$$

One should note that the NLOS path length error in (9) is correct when the electromagnetic wave is orthogonal to the obstacle. It is possible to refine the path length estimate corrections by taking account of the angles of passage of electromagnetic waves through obstacles. For example, by taking refraction into account, an UWB wave traveling from point A through a wall to point B is illustrated in Fig. 2.

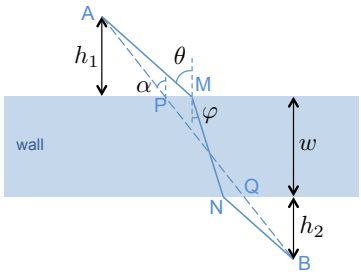

Fig. 2. Refraction of UWB waves through a wall.

Then, the NLOS path length estimation error is given by

$$n_\tau = \mathrm{AM} + \mathrm{MN}\sqrt{\varepsilon_r \mu_r} + \mathrm{NB} - \mathrm{AB} = \frac{h}{\cos\theta} + \frac{w}{\cos\varphi}\sqrt{\varepsilon_r \mu_r} - \frac{h + w}{\cos\alpha}, \quad (10)$$

where $h = h_1 + h_2$, α is the intersection angle between the direct path and the wall, θ and φ are respectively the angles of incidence and refraction. It is well known that the relationship

between θ and φ is described by Snell's law of refraction, i.e. $\sin\theta/\sin\varphi = \sqrt{\varepsilon_r\mu_r}$. However the derivation of the equation relating θ to α, h_1, h_2 and w is not straightforward, and the resulting equation cannot be solved in closed form, especially when UWB waves travel through multiple walls with different intersection angles.

Lemma 1: When an UWB wave travels through a wall with $\varepsilon_r\mu_r > 1$, thickness w and intersection angle α, the error on the NLOS path length estimation is bounded by

$$w(\sqrt{\varepsilon_r\mu_r - \sin^2\alpha} - \cos\alpha) \le n_\tau \le \frac{w}{\cos\alpha}(\sqrt{\varepsilon_r\mu_r} - 1) \quad (11)$$

Proof: See Appendix. □

It is noted that the lower bound of NLOS path length error is obtained with $\theta \to \alpha$, in other words, $h \gg w$. In reality, the distance between the Tag and the Anchor is much greater than the thickness of wall, therefore we can simplify the form of NLOS path length error by its lower bound.

Lemma 2: The NLOS path length error is minimum if and only if the UWB wave travels orthogonally to the wall.

Proof: upon differentiation, we find that the upper and lower bounds in (11) are strictly increasing functions of α, and both are equal to (9) for $\alpha = 0$. □

In Sigma Laboratory, as an example, the NLOS path length estimation error for a signal traversing orthogonally to a 10-cm thick wall with $\mu_r = 1$ and $\varepsilon_r = 7$ is approximately 16 cm. That this property is indeed obeyed in our UWB ranging context will be confirmed in the results Section IV-A.

B. Proposed method

Due to the influence of NLOS propagation in indoor localization, the equation in (3) must be replaced by

$$r_i \ge f_i + e_i + n_i, \quad (12)$$

where n_i is the minimum possible NLOS path length estimation error on a path from the source to the i^{th} receiver. Then, the optimization problem to solve is

$$\min\left\{(\mathbf{h} - \mathbf{G}\boldsymbol{\delta})^T\mathbf{R}^{-1}(\mathbf{h} - \mathbf{G}\boldsymbol{\delta})\right\}, \text{ such that } \mathbf{G}\boldsymbol{\delta} \le \mathbf{h} - \mathbf{n}, \quad (13)$$

with $\mathbf{n} = [n_1, n_2, ..., n_N]^T$. A method to solve this quadratic programming problem is given in [12]; however, here, the exact value of n_i is unknown.

In this paper, a simple method for indoor localization including the contribution of NLOS signals is proposed. The key idea is that if the Tag position and the map layout are known, one may determine the number of obstacles (concrete walls, in the present case) in the 2-D floor plan traversed by the signal in a straight line, at normal incidence, from Tag to Anchor. Assuming that signals reflected by obstacles have no influence on the received signal at the i^{th} Anchor, the NLOS path length error is then approximated by

$$n_i = \sum_{k\in\mathcal{D}_i} w_{k,i}(\sqrt{\varepsilon_r\mu_r - \sin^2\alpha_{k,i}} - \cos\alpha_{k,i}), \quad (14)$$

Input:
$\mathcal{P}$: set of Anchor position vectors $\mathbf{p}_i = [x_i, y_i]^T$,
$\mathbf{R}$: covariance matrix of the estimation error $\mathbf{e}$,
$\mathbf{r}$: vector of observed distances.
Output:
$\hat{\mathbf{p}}$: position estimate.
function POSEST($\mathcal{P}, \mathbf{R}, \mathbf{r}$)
  Sort all of the distances r_i in decreasing order.
  Choose N shortest distances for localization.
  Compute the initial position $\hat{\mathbf{p}} = \hat{\mathbf{p}}_0$ (using [13]).
  do ▷ *start iteration*
    Define intersections with obstacles using [14].
    $n_i \leftarrow \sum_{k\in\mathcal{D}_i} w_{k,i}(\sqrt{\varepsilon_r\mu_r - \sin^2\alpha_{k,i}} - \cos\alpha_{k,i})$.
    $f_i \leftarrow \sqrt{(x - x_i)^2 + (y - y_i)^2}$.
    Compute matrices $\mathbf{G}$, $\mathbf{h}'$ using (6), (17).
    $\boldsymbol{\delta} \leftarrow \left(\mathbf{G}^T\mathbf{R}^{-1}\mathbf{G}\right)^{-1}\mathbf{G}^T\mathbf{R}^{-1}\mathbf{h}'$.
    $\hat{\mathbf{p}} \leftarrow \hat{\mathbf{p}} + \boldsymbol{\delta}$.
    if $\Phi_{\min} \ge \mathbf{h}'^T\mathbf{R}^{-1}\mathbf{h}'$ **then**
      $\Phi_{\min} \leftarrow \mathbf{h}'^T\mathbf{R}^{-1}\mathbf{h}'$
      $\hat{\mathbf{p}}_{\min} \leftarrow \hat{\mathbf{p}}$
    end if
  while $\|\boldsymbol{\delta}\| \le \epsilon$ or $N_{\text{iter}} \ge$ const ▷ *end iteration*
  return $\hat{\mathbf{p}} = \hat{\mathbf{p}}_{\min}$
end function

Fig. 3. Outline of the proposed positioning algorithm.

where $w_{k,i}$ is the thickness, and $\alpha_{k,i}$ is the intersection angle of the k^{th} wall with the direct path $\mathcal{D}_i$ from the Tag to the i^{th} Anchor. Here, we assume that all of the walls have the same permeability and permittivity. If the thicknesses of these walls are also the same, and the direct path is orthogonal to all of them, one has

$$n_i = \mathcal{N}_i w\left(\sqrt{\varepsilon_r\mu_r} - 1\right), \quad (15)$$

where $\mathcal{N}_i$ is the number of walls on the path from the Tag to the i^{th} Anchor. For simplicity, it is assumed that the inequalities in (12) become equalities, so that the vector $\boldsymbol{\delta}$ in (13) is given by

$$\boldsymbol{\delta} = \left(\mathbf{G}^T\mathbf{R}^{-1}\mathbf{G}\right)^{-1}\mathbf{G}^T\mathbf{R}^{-1}\mathbf{h}', \quad (16)$$

where

$$\mathbf{h}' = \mathbf{h} - \mathbf{n} = \begin{bmatrix} r_1 - f_1 - n_1 \\ \vdots \\ r_N - f_N - n_N \end{bmatrix}. \quad (17)$$

Using these approximations, the proposed positioning algorithm is shown in Fig. 3. At each iteration of the nonlinear least squares algorithm, the NLOS path length errors n_i are estimated by intersections between the direct paths from current position to the i^{th} Anchor and the walls in the floor plan which are modeled as line segments [14]. Since this NLOS estimation correction is applied at each iteration of the Taylor expansion, the computational complexity of the approach does not increase beyond that of the Taylor approximation loop

itself. However, one should note that this method requires a close enough starting point to guarantee convergence. To this end, the linear algorithm proposed in [13] is used to determine the initial position (under the assumption that there are no NLOS path length errors). Furthermore, in order to improve the convergence, the value of $\Phi = \mathbf{h}'^T \mathbf{R}^{-1} \mathbf{h}'$ is computed at each iteration, and the estimated position is taken to be the position for which Φ is minimum.

IV. Experiments and Results

A. NLOS path length estimation error tests

Firstly, the performance of the proposed UWB ranging system in the indoor environment with multiple concrete walls is validated. Fig. 4 shows the TWR-estimated distances between a Tag and an Anchor separated by 3m. When no obstacles are between them, the magnitude of the mean ranging error is about 6.7 cm. The fluctuation of the ranging distances and the LOS path length estimation error can be explained by the influence of the clock offset on the UWB transmitter and receiver, see [15]. When there is one concrete wall of 10 cm thickness between the Tag and the Anchor, the magnitude of the mean ranging error rises to 23.5 cm. The NLOS path length estimation error in this case is therefore about 16.8 cm, due to the reduced velocity of the electromagnetic wave in the concrete wall. Ranging errors conform to a Gaussian distribution $\mathcal{N}(e_0, \sigma_e^2)$, where the standard deviation σ_e is related to the UWB system parameters, see [16]. It may be conjectured that the decrease of the variance in the NLOS case as compared to the LOS case is due to the reduction of some NLOS signals reflected by other walls.

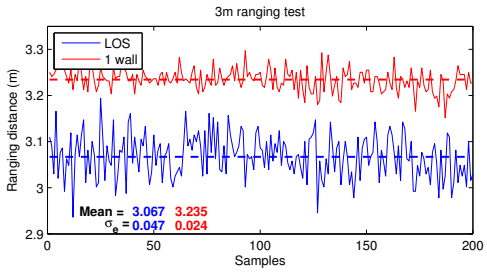

Fig. 4. Ranging results for the distance of 3 m.

The performance of NLOS path length estimation for multiple concrete walls of the same thickness, 10 cm, is illustrated in Fig. 5. It is observed that, in the range that was investigated experimentally, the error increases linearly with the number of walls. This validates the algorithm proposed in Section III-B. In the following, we assume that the NLOS path length estimation error is 16 cm for one wall.

B. Simulation results

In the simulation reported here, it is assumed that there are four Anchors at the corners of a horizontal 8 m by 6 m rectangle, that the Tag is at the center of the rectangle (see Fig. 6), and that the direct path from the Tag to the fourth Anchor is obstructed by a concrete wall. It is also assumed that the

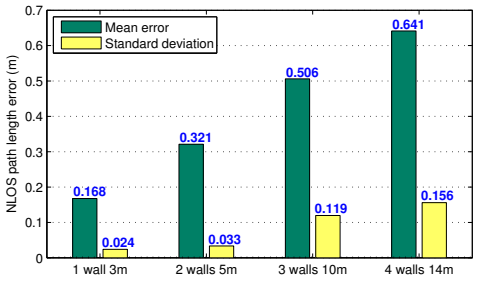

Fig. 5. NLOS path length estimation errors for different numbers of walls.

ranging errors of LOS paths follow a Gaussian distribution $\mathcal{N}(0.07, 0.05^2)$, or for an NLOS path with one concrete wall, $\mathcal{N}(0.23, 0.05^2)$. The NLOS path length error in this case is therefore 16 cm.

Fig. 6.a shows the simulation result of 300 measurements collected at the position (4m, 3m), without using the NLOS path length estimation error correction algorithm. In this figure, the box on the left is a zoom of all estimated positions found in the rectangle at the center of the figure. It is seen that the located positions are shifted down and to the left from the true position denoted by the blue asterisk. This is due to the influence of the NLOS path length estimation error from the fourth Anchor at the top right corner, which leads to an overestimation of the tag-to-anchor distance. If only three LOS Anchors are used to locate the position of the Tag, it can be seen from Fig. 6.b that the estimated positions are shifted to top-right due to the LOS ranging estimation error of 7 cm. The mean location errors (MLEs), i.e. the mean value of the Euclidean distances between the estimated positions and the true position of the Tag, are respectively 9.1 cm and 8.8 cm in these two cases. In contrast, the cluster of 300 positions estimated by the proposed method is centered on the true position, as illustrated in Fig. 6.c. The mean location error is now about 4.5 cm, which is two times smaller than the case of the LOS algorithms

Next, it is assumed that the Tag has uniformly distributed random positions inside the rectangle defined by the four Anchors above, i.e. $0 \leq x \leq 8$ m and $0 \leq y \leq 6$ m. It is to be expected that the actual mean LOS ranging estimation error will vary with position; here we assume it varies uniformly between 0 and 7 cm. For NLOS paths a further fixed value of 16 cm is added to the length estimation error. Fig. 7 shows the performance of MLE, obtained from 30000 independent runs, with respect to the standard deviation of the ranging error. One observes that the performance of our NLOS estimation error correction method is better than the LOS estimations. Moreover, this improvement is more significant when the standard deviation increases. Fig. 8 illustrates the effect of the magnitude of NLOS path length error on the MLE performance. Herein, different numbers of walls between the Tag and the NLOS Anchor are considered, and we assumed that the standard deviation of the estimation error is proportional to the number of walls. A t-test was used to confirm that the proposed method significantly outperforms the LOS algorithms.

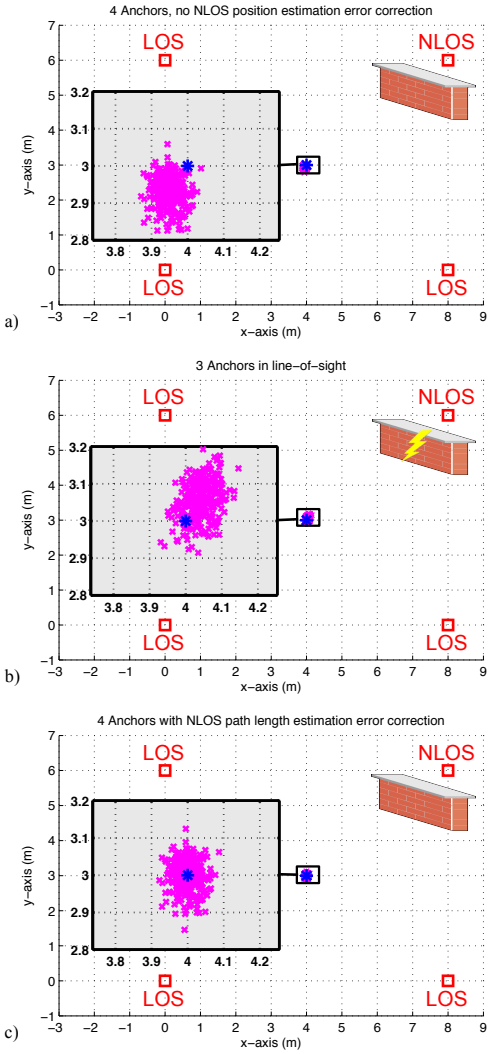

Fig. 6. Comparing the estimated positions: (a) using LOS algorithm, (b) eliminating the NLOS Anchor, and (c) using the proposed method. The red squares denote the positions of the Anchors; the blue star denotes the position of the Tag.

C. Experimental results

Experiments were performed at the Sigma Laboratory at ESPCI ParisTech, in Paris, France. The laboratory is approximately 24×17 m in size and consists of rooms and corridors separated by concrete walls. Anchors are fixed at known locations in a relative coordinate system, these relative positions of Anchors being determined using a standard metallic tape measure. Fig. 9 shows an example set of 30 measurements collected at a random position in room H4.18. In this figure, the Anchors are denoted by red square symbols, and the true position of the Tag by the blue symbol. It is seen that the estimated positions using the proposed method in Section III-B are more accurate than those using the LOS algorithm. Indeed, the mean location error obtained by NLOS algorithm is about 54 cm, as compared with 99 cm for the LOS algorithm.

Table I shows the mean location errors for all experiments with Tag placed randomly in Sigma Laboratory. When there is no NLOS path between the Tag and the Anchors, the MLE performances of both methods are the same and rather good at about 19 cm. However, when there exist NLOS paths, the experiments confirm a significant improvement in MLE using the proposed NLOS error correction algorithm.

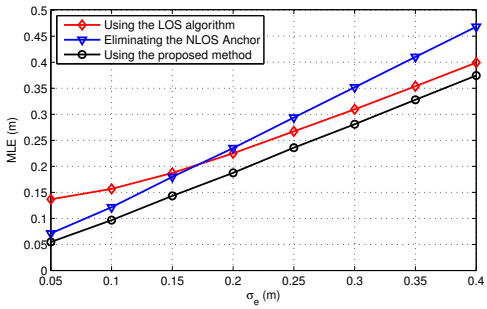

Fig. 7. Effect of the standard deviation of the ranging error on MLE performance.

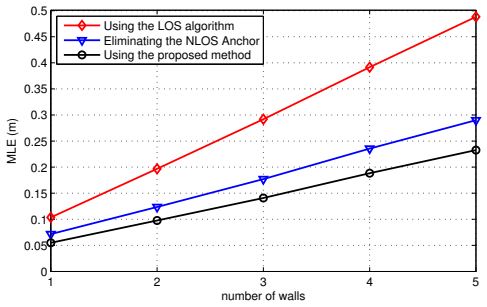

Fig. 8. Effect of the number of walls on MLE performance.

TABLE I
COMPARISON OF MLES FOR ALL RECORDINGS

Algorithm	**0 NLOS** (cm)	**1 NLOS** † (cm)	**2 NLOS** † (cm)	**3 NLOS** † (cm)
LOS	19	49	117	162
Proposed	19	25	45	57

† Numbers of links to 3 anchors are in NLOS conditions, many wall penetrations may occurred on each link.

V. CONCLUSIONS

A positioning algorithm to reduce the NLOS errors for indoor localization systems has been presented. In laboratory experiments, the NLOS path length estimation error is shown to increase linearly with the number of concrete walls traversed in a linear path from source to receiver. By correcting the NLOS delays in the propagation of the UWB signal using the physics of wave propagation on each iteration of the proposed algorithm, a significant improvement of accuracy is obtained in comparison with the LOS algorithm. Tests in Sigma Laboratory demonstrated a reduction about 50% of the mean location error. A limitation of the proposed algorithm is that, in practice, the actual propagation delay will depend on such factors as the true material composition, form, and the thickness of obstacles encountered, which may be difficult to ascertain a priori.

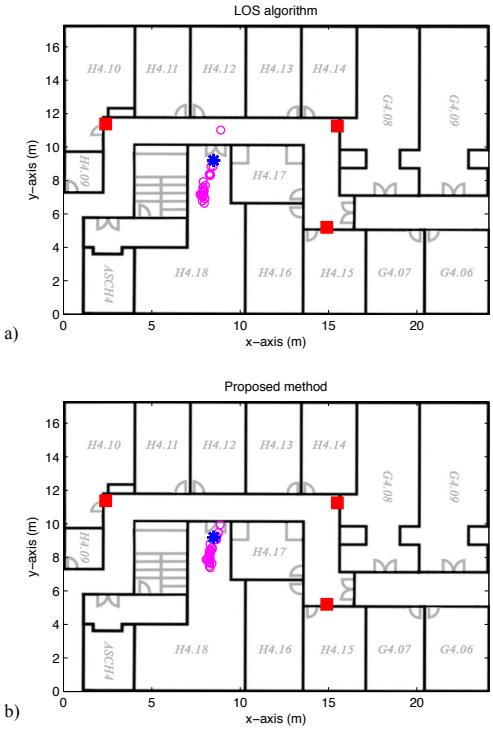

Fig. 9. Experiments collected in Sigma laboratory: (a) using the LOS algorithm, and (b) using proposed method.

APPENDIX
PROOF OF LEMMA 1

Firstly, we point out the upper bound of NLOS path length estimation error. In the Fig. 2, according to Fermat's principle, i.e. the path taken between two points by an electromagnetic wave is the path that can be traversed in the least time, so we have

$$\mathrm{AM} + \mathrm{MN}\sqrt{\varepsilon_r\mu_r} + \mathrm{NB} \le \mathrm{AP} + \mathrm{PQ}\sqrt{\varepsilon_r\mu_r} + \mathrm{QB}. \quad (18)$$

By substituting (18) to (10), we obtain

$$n_\tau \le \mathrm{PQ}\sqrt{\varepsilon_r\mu_r} - \mathrm{PQ} = \frac{w}{\cos\alpha}(\sqrt{\varepsilon_r\mu_r} - 1). \quad (19)$$

For $\pi/2 \ge \theta$, we have the following inequality

$$\frac{1}{\cos\theta} \ge \frac{\cos(\theta-\alpha)}{\cos\theta} = \frac{\sin\theta\sin\alpha + \cos\theta\cos\alpha}{\cos\theta} =$$
$$= \tan\theta\sin\alpha + \cos\alpha = \tan\theta\sin\alpha + \frac{1}{\cos\alpha} - \tan\alpha\sin\alpha$$

or

$$\frac{h}{\cos\theta} - \frac{h}{\cos\alpha} \ge h(\tan\theta - \tan\alpha)\sin\alpha. \quad (20)$$

Moreover, from Fig. 2, we have the following relationship

$$MP + NQ = h(\tan\theta - \tan\alpha) = w(\tan\alpha - \tan\varphi). \quad (21)$$

By substituting (20) and (21) to (10), we obtain

$$n_\tau \ge w\left(\frac{\sqrt{\varepsilon_r\mu_r}}{\cos\varphi} - \frac{1}{\cos\alpha} + (\tan\alpha - \tan\varphi)\sin\alpha\right)$$
$$\ge w\left(\frac{\sqrt{\varepsilon_r\mu_r} - \sin\alpha\sin\varphi}{\cos\varphi} - \cos\alpha\right) \quad (22)$$

Comparing (22) with the lower bound in (11), it must be proved that

$$\frac{\sqrt{\varepsilon_r\mu_r} - \sin\alpha\sin\varphi}{\cos\varphi} \ge \sqrt{\varepsilon_r\mu_r - \sin^2\alpha}. \quad (23)$$

Indeed, multiplying by $\cos\varphi$, and squaring both sides, one gets

$$(\sqrt{\varepsilon_r\mu_r} - \sin\alpha\sin\varphi)^2 - \cos^2\varphi(\varepsilon_r\mu_r - \sin^2\alpha) =$$
$$(\sqrt{\varepsilon_r\mu_r}\sin\varphi - \sin\alpha)^2 \ge 0. \quad (24)$$

Because $\sqrt{\varepsilon_r\mu_r} > 1 \ge \sin\alpha\sin\varphi$, so inequality (23) is satisfied. It is thus proved that

$$n_\tau \ge w(\sqrt{\varepsilon_r\mu_r - \sin^2\alpha} - \cos\alpha). \quad (25)$$

One should note that the lower and upper bounds of NLOS path length error hold for $\theta \to \alpha$ and $\varphi \to \alpha$, in respectively.

REFERENCES

[1] M. Scherhaufl, M. Pichler, E. Schimback, D. Muller, A. Ziroff, and A. Stelzer, "Indoor localization of passive UHF RFID tags based on phase-of-arrival evaluation," *IEEE Transactions on Microwave Theory and Techniques*, vol. 61, no. 12, pp. 4724–4729, Dec 2013.

[2] K. Wu, J. Xiao, Y. Yi, D. Chen, X. Luo, and L. Ni, "CSI-based indoor localization," *IEEE Transactions on Parallel and Distributed Systems*, vol. 24, no. 7, pp. 1300–1309, July 2013.

[3] J. Diaz, R. de A Maues, R. Soares, E. Nakamura, and C. Figueiredo, "Bluepass: An indoor bluetooth-based localization system for mobile applications," in *IEEE Symposium on Computers and Communications (ISCC)*, June 2010, pp. 778–783.

[4] Z. Sahinoglu, S. Gezici, and I. Guvenc, *Ultra-wideband positioning systems*. Cambridge, New York, 2008.

[5] T. Gigl, G. Janssen, V. Dizdarevic, K. Witrisal, and Z. Irahhauten, "Analysis of a UWB indoor positioning system based on received signal strength," in *4th Workshop on Positioning, Navigation and Communication, 2007. WPNC '07.*, March 2007, pp. 97–101.

[6] I. Guvenc, Z. Sahinoglu, and P. Orlik, "TOA estimation for IR-UWB systems with different transceiver types," *IEEE Transactions on Microwave Theory and Techniques*, vol. 54, no. 4, pp. 1876–1886, June 2006.

[7] J. Xu, M. Ma, and C. Law, "AOA cooperative position localization," in *Global Telecommunications Conference, 2008. IEEE GLOBECOM 2008.*, Nov 2008, pp. 1–5.

[8] W. Suski, S. Banerjee, and A. Hoover, "Using a map of measurement noise to improve UWB indoor position tracking," *IEEE Transactions on Instrumentation and Measurement*, vol. 62, no. 8, pp. 2228–2236, 2013.

[9] I. Guvenc and C.-C. Chong, "A survey on TOA based wireless localization and NLOS mitigation techniques," *IEEE Communications Surveys Tutorials*, vol. 11, no. 3, pp. 107–124, rd 2009.

[10] DecaWave. DW1000 data sheet. Dublin, Ireland. [Online]. Available: http://www.decawave.com/support

[11] D. Dardari, A. Conti, U. Ferner, A. Giorgetti, and M. Win, "Ranging with ultrawide bandwidth signals in multipath environments," *Proceedings of the IEEE*, vol. 97, no. 2, pp. 404–426, Feb 2009.

[12] R. Fletcher, "A general quadratic programming algorithm," *IMA Journal of Applied Mathematics*, vol. 7, no. 1, pp. 76–91, 1971.

[13] J. J. Caffery Jr, "A new approach to the geometry of TOA location," in *Vehicular Technology Conference, 2000. IEEE-VTS Fall VTC 2000. 52nd*, vol. 4, 2000, pp. 1943–1949.

[14] M. De Berg, M. Van Kreveld, M. Overmars, and O. C. Schwarzkopf, *Computational geometry (2nd edition)*. Springer, 2000, ch. 2: Line Segment Intersection.

[15] T. Ye, M. Walsh, P. Haigh, J. Barton, and B. O'Flynn, "Experimental impulse radio ieee 802.15. 4a UWB based wireless sensor localization technology: Characterization, reliability and ranging," in *22nd IET Irish Signals and Systems Conference, Dublin, Ireland.*, Jun 2011.

[16] Y. Qi, H. Kobayashi, and H. Suda, "Analysis of wireless geolocation in a non-line-of-sight environment," *IEEE Transactions on Wireless Communications*, vol. 5, no. 3, pp. 672–681, 2006.